ELSEVIER

Journal of Crystal Growth 230 (2001) 270–276

JOURNAL OF CRYSTAL GROWTH

www.elsevier.com/locate/jcrysgro

Simulations of crystallization and melting of the FCC (1 0 0) interface: the crucial role of lattice imperfections

H.L. Tepper[a,*], W.J. Briels[b]

[a] *Computational Chemistry Group, University of Twente, P.O. Box 217, 7500 AE Enschede, Netherlands*
[b] *Computational Dispersion Rheology, University of Twente, P.O. Box 217, 7500 AE Enschede, Netherlands*

Abstract

We present nonequilibrium simulations of growth and melting of the atomic FCC (1 0 0) interface. Using Nosé–Hoover dynamics we have carefully studied size effects and approximated the dynamics of the solid–liquid interface in a large system as closely as possible. This led to a clear asymmetry of growth and melting rates close to equilibrium. It was possible to explain these findings in terms of the lattice imperfections in crystalline phases in contact with a liquid phase, which automatically developed during growth simulations but were absent in the melting simulations. It was shown that when melting simulations were started with appropriate starting configurations, the asymmetry could be made to disappear.

PACS: 81.10.Aj; 64.70.Dv; 71.15.Pd

Keywords: A1. Computer simulation; A1. Defects; A1. Growth models; A1. Interfaces; A1. Solidification; A2. Growth from melt

1. Introduction

Although much is known about the thermodynamics of the solid–liquid phase transition, the kinetics of this transition is still poorly understood. Part of this is due to the fact that, being a combination of two dense phases, the crystal–melt interface is not easily accessible to experiment. Therefore, computer simulations can be of great help in understanding the microscopic processes involved in crystallization or melting. Over the past few years, excellent reviews have appeared on computer modelling and on theories of the structure and dynamics of the crystal–liquid interface [1–3].

Most crystallization and melting processes are heterogeneous, i.e. they involve the motion of an interface throughout the system. Among the first to make an extensive study of this process, were Broughton et al. [4–7]. They combined the solid and the liquid phase in one simulation box and calculated growth rates over a wide range of temperatures. They, however, did not study melting.

In an earlier paper of ours [8], we studied the steady state velocity of the interface in a Lennard-Jones system at small undercoolings and superheatings. We established growth and melting rates as a function of the deviation from equilibrium by

*Corresponding author. Tel.: +31-53-489-4039; fax: +31-53-489-2799.

E-mail addresses: h.l.tepper@ct.utwente.nl (H.L. Tepper), w.j.briels@tn.utwente.nl (W.J. Briels).

0022-0248/01/$ - see front matter
PII: S0022-0248(01)01339-2

performing several nonequilibrium simulations. On the basis of Onsager's regression hypothesis, we were able to obtain the same information from fluctuations of the amount of crystalline material during one single equilibrium simulation. In a recent study we successfully applied the same (universal) procedure to the calculation of transport diffusion of guest molecules in a zeolite [9].

Over the past 15 years, much debate has evolved on the question whether the interface response should be symmetric around the equilibrium temperature. An argument on the basis of microscopic reversibility, already presented in the 1960s [10], concluded that if molecules are added to or taken from similar interface sites, then the curves of crystallization rate and melting rate versus temperature should be continuous with the same slope through the melting temperature. The debate was initiated again, however, by Tsao et al. [11] who reported experiments of laser-induced zone melting of silicon, in which growth of the melt into the superheated solid appeared to be much faster than growth of the crystal into the undercooled liquid. Since they dealt with large deviations from equilibrium, no sharp conclusion can be drawn about a possible slope discontinuity at equilibrium.

Kluge and Ray [12] performed molecular dynamics simulations of crystallization and melting of silicon. They employed a Stillinger–Weber potential and considered large deviations from equilibrium. Their results show the same trends as the experiments by Tsao. Tymczak and Ray [13] performed similar simulations on sodium crystals having BCC symmetry. They found a clear slope discontinuity at equilibrium with melting being substantially faster than crystallization. However, since they mimic the electron density dependence of the interactions by changing the potential with temperature, it is impossible in this case also to draw any conclusions about the occurrence of an asymmetry between growth and melting rate in systems interacting via Lennard-Jones potentials.

The only careful investigation at small undercoolings and superheatings was presented by Moss and Harrowell [14]. They performed dynamic Monte Carlo simulations of the FCC lattice gas and studied freezing and melting of the simple cubic phase. Besides a clear slope discontinuity, they also found a small range of supercoolings where the growth velocity essentially vanished.

From all of the above, no clear picture arises of the possibility or impossibility of a slope discontinuity in the interface response near equilibrium. In the present paper, we will present detailed measurements of the growth and melting rates in an atomistic simulation and will address some of the subtleties that arise in performing such simulations. We will show that a slope discontinuity arises when starting growth and melting simulations from well equilibrated liquid and solid phases. The discontinuity will be seen to disappear only when lattice imperfections occurring in rapidly growing crystals are also taken into account in the melting simulations.

2. Interaction model

To avoid possible complications with long-range attractions (which would lead to different long-range corrections in bulk and two-phase systems), we required a pair potential which is exactly zero beyond a certain cut-off radius. To this end, we employed the shifted force $12-6$ potential as introduced by Clarke et al. [15] (where it has the general form of an $n-m$ potential). The potential has the following structure:

$$U(r_{ij}) = \alpha\varepsilon\left[\beta^{12}\left\{\left(\frac{r_0}{r_{ij}}\right)^{12} - \left(\frac{1}{\gamma}\right)^{12}\right\} - 2\beta^6\left\{\left(\frac{r_0}{r_{ij}}\right)^{6} - \left(\frac{1}{\gamma}\right)^{6}\right\}\right] + 12\alpha\varepsilon\left(\frac{r_{ij}-\gamma r_0}{\gamma r_0}\right)\left\{\left(\frac{\beta}{\gamma}\right)^{12} - \left(\frac{\beta}{\gamma}\right)^{6}\right\} \quad (1)$$

with

$$\gamma = \frac{r_{\mathrm{cut}}}{r_0}, \quad (2)$$

$$\beta = \gamma\left(\frac{\gamma^7 - 1}{\gamma^{13} - 1}\right)^{1/6} \quad (3)$$

and

$$\alpha = [2\beta^6(1 + (6 - 7\gamma)/\gamma^7) - \beta^{12}(1 + (12 - 13\gamma)/\gamma^{13})]^{-1}. \quad (4)$$

This form has the advantage over the standard shifted force potentials that both ε and r_0 (the well depth and the location of the minimum) retain their original meaning after the shifting process. In our simulations we will take the common value $r_{\text{cut}} = 2.5\sigma$ where σ is implicitly defined by $r_0 = 2^{1/6}\sigma$. All properties will be presented in terms of ε, σ, and the mass m (common Lennard-Jones units).

3. Simulation method

We performed molecular dynamics simulations at constant number of particles (N), constant pressure (P), and constant temperature (T). In order to simulate a true isothermal–isobaric ensemble, we used Nosé–Hoover dynamics [16,17] to integrate the equations of motion, in which the thermostat and barostat variables are taking part in the dynamics of the system. We made a careful study of pressure and temperature distributions in a bulk liquid and bulk solid in order to tune the thermostat and barostat relaxation times so as to ensure that the distributions had the correct width within reasonable simulation time and that the pressure and temperature fluctuations did not interact. This resulted in $\tau_T = 0.0748\ \sigma\sqrt{m/\varepsilon}$ and $\tau_P = 0.748\ \sigma\sqrt{m/\varepsilon}$, with a timestep of $\Delta t = 0.000748\ \sigma\sqrt{m/\varepsilon}$.

In order to derive the correct temperature dependence of the bulk densities, we performed NPT simulations on bulk systems of liquid (512 particles) and FCC solid (500 particles) at various temperatures and pressure $P = 0.0025\ \varepsilon/\sigma^3$. Average volumes were calculated over 200 000 timesteps. The volumes per atom were least-squares fitted to a straight function in T resulting in

$$v_l^* = 0.76111 + 0.77153 \times T^*, \quad 0.580 < T^* < 0.630 \quad (5)$$

and

$$v_s^* = 0.85370 + 0.35466 \times T^*, \quad 0.580 < T^* < 0.630. \quad (6)$$

With the fitted volumes, new bulk simulations were performed at constant volume. The solid and liquid boxes were made such that they had the same cross section in the x, y-plane. The bulk NVT simulations were run for 100 000 timesteps of equilibration, whereafter co-ordinate files were written every 10 000 timesteps. To make two-phase boxes, one liquid configuration and one solid configuration were taken, both copied four times in the z-direction, and subsequently put on top of each other. This way, two interfaces appear in the boxes, with their surfaces along the x- and y-axes. The resulting boxes consisted of 2000 initially crystalline particles ($5 \times 5 \times 20$ unit cells) and 2048 particles initially belonging to the liquid phase. To release excessive potential energies due to particle overlap, 300 timesteps of NVT simulations were performed with rigid temperature scaling at every timestep. After this, NPT runs were carried out to study growth and melting rates. The pressure scaling routine was adopted such that the volume relaxation in x-, y-, and z-directions took place independently.

4. Results

In order to calculate the growth and melting rates, we used an order parameter to distinguish the crystal phase from the liquid phase. The order parameter, which was introduced in Ref. [8], takes advantage of the octahedral symmetry of the nearest neighbours around a particle in an FCC crystal. As can be seen in that paper, a function Ψ could be derived which discriminates very well between 'solid-like' and 'liquid-like' particles. The advantage of the order parameter is that it is defined for each atom; so keeping track of the growth of one phase comes down to merely counting the number of particles belonging to the crystal.

Results of growth and melting simulations are presented in Fig. 1. Each curve stands for the average of 50 simulations at a given temperature.

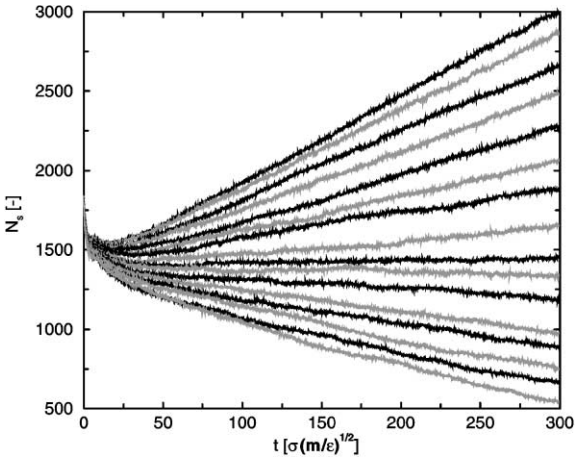

Fig. 1. Growth and melting curves from nonequilibrium simulations showing the number of solid-like particles versus time. Results are shown for a range of temperatures varying from 0.580 $\sigma\sqrt{m/\varepsilon}$ (upmost curve) to 0.630 $\sigma\sqrt{m/\varepsilon}$ (lowest curve).

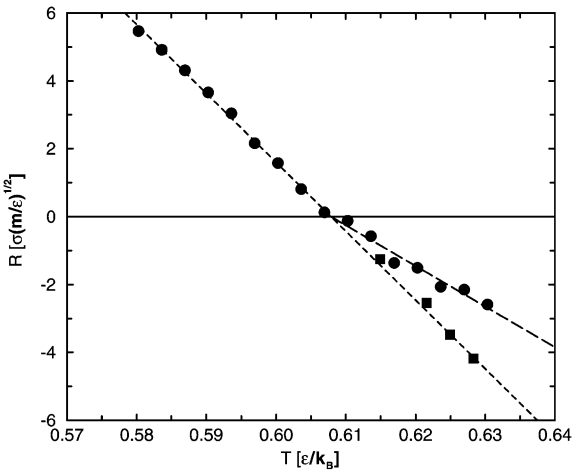

Fig. 2. Temperature dependence of growth and melting rates. A clear asymmetry is seen between growth and melting rates from the old method (filled circles). Rates from melt simulations where lattice imperfections were taken into account are shown as filled squares.

Due to the substantial temperature fluctuations in the isothermal–isobaric ensemble, a spreading naturally arises in the results from different runs at the same temperature. Therefore, several runs with different initial configurations (combinations of different configurations from the solid as well as from the liquid runs) had to be carried out to obtain good statistical accuracy. As can be seen from the figure, the overall behaviour is universal; after an equilibration period of less than 50 reduced time units, the number of crystalline particles increases or decreases linearly in time. This means that the supersaturation was kept constant and the two interfaces were separated far enough so as to not interact with one another.

Note that our system size is substantially larger (a factor 2.5) than the one used by Broughton et al. [6]. Their claim that their interfaces did not interact was underpinned by checking only static bulk properties and not dynamic properties. We found that with a system of half the present size, the region before the constant linear regime really sets in is almost twice as long, making it much harder to measure the growth rates accurately.

An alternative way of measuring growth rates is by monitoring the volume evolution of the system in time. The number of crystal particles at time t can then be estimated by

$$N_s(t) = \frac{N_{\text{total}} \times v_l - V_{\text{total}}(t)}{v_l - v_s}. \tag{7}$$

The results of both methods for $T = 0.580\ \varepsilon/k_{\text{B}}$ are similar. This implies that the density front in the simulation is moving at the same speed as the order front. This holds true for all temperatures we investigated.

From the linear part of the growth curves, growth rates were calculated and plotted versus temperature in Fig. 2 (filled circles). As can be seen from the figure, this procedure led to an apparent asymmetry of the growth and melting rates in the vicinity of the equilibrium point. We checked whether this asymmetry was independent of the vertical box size, by performing simulations of boxes of half the size. Moreover, since volume measurements and order parameter measurements gave the same results, we concluded that the asymmetry was not an artifact of the measurement method.

There was one feature of the method which was inherently asymmetric and, therefore, might be the cause of the asymmetry. That is, the crystals emerging from the growth simulations had incorporated certain imperfections which were not

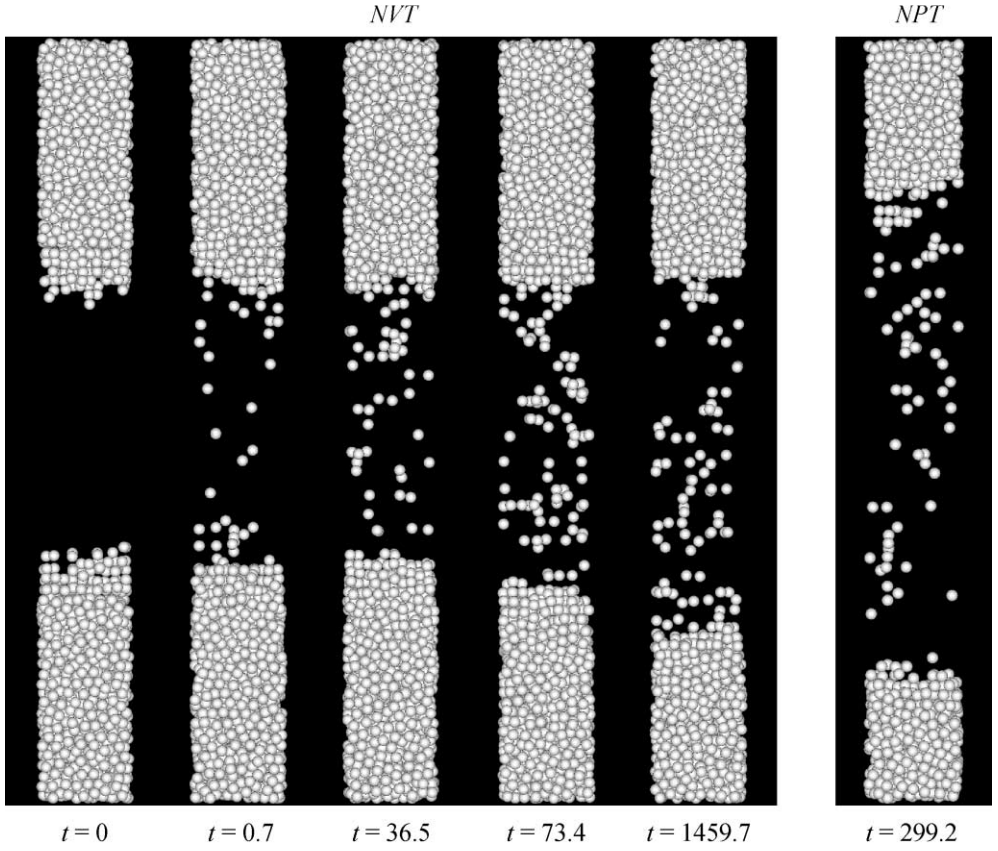

Fig. 3. Snapshots of different stages in an equilibrium run (NVT) and of an end configuration of a nonequilibrium run (NPT) at $T = 0.587\ \sigma\sqrt{m/\varepsilon}$. Only the particles classified as 'liquid-like' are shown, providing a clear representation of the amount of mismatch in the crystalline lattice.

present in the bulk crystals. When looking at Fig. 3, where only the disordered ('liquid-like') particles have been drawn, one sees that the crystal at the end of a growth simulation (denoted with NPT) contains imperfections. An example of a starting configuration of a two-phase run (containing an equilibrated solid in the middle) is shown in the first snapshot of Fig. 3, which indeed shows no liquid-like particles in the crystalline phase. Unlike the discussion of imperfections by others like Burke et al. [7] and Huitema et al. [18], almost all of these imperfections were interstitial atoms, not vacancies. Virtually all layers contained the maximum amount of particles, i.e. 50 (which was easily checked by integrating the longitudinal density profile layer by layer), but, on average, one particle per layer was located away from its lattice site. Burke et al. reported a substantial increase of the vacancy concentration upon decreasing temperature. Unfortunately, they did not explain the way they measured the vacancy concentration. Again, it should be noted that they investigated much larger undercoolings than we did. Huitema et al. reported on undercoolings comparable to ours, but their results suffer from poor statistics and they also do not explain their way of quantification of the number of vacancies.

Since it is now clear that the crystals grown below equilibrium are structurally different from the crystals with which we started our melting simulations, the asymmetry might be explained by this difference. In order to check this we took the 50 end configurations at a certain temperature and started new simulations therewith at temperatures

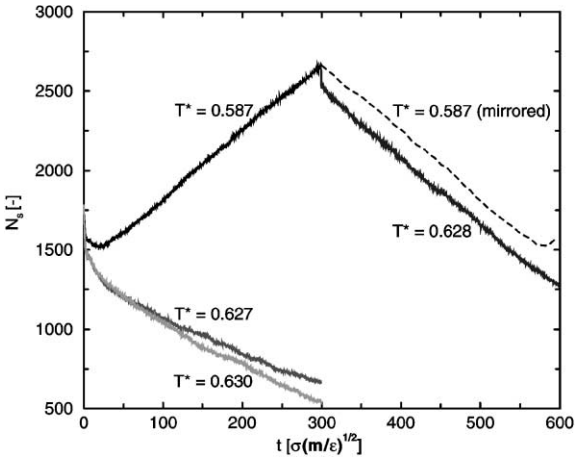

Fig. 4. Growth and melting curves showing the difference between starting from configurations with and without lattice imperfections in the crystalline phase.

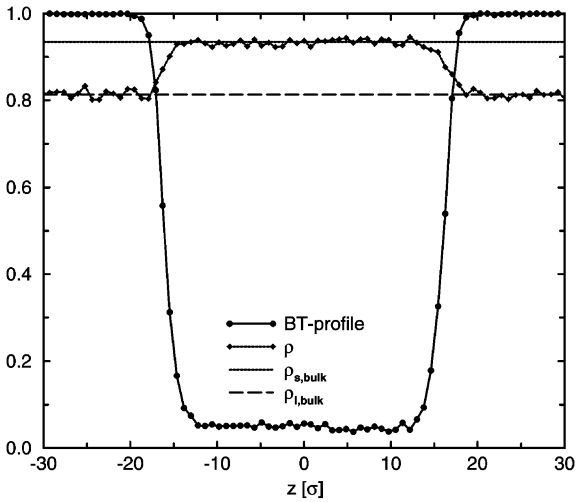

Fig. 5. Laterally integrated density and order profile in an equilibrium simulation.

at the same amount of superheating as the amount of undercooling at which they were produced. In other words, the systems were put on the mirror side of the equilibrium temperature (which was estimated from Fig. 2 to be $0.608\ \sigma\sqrt{m/\varepsilon}$). The result of one such experiment is shown in Fig. 4. As a guide, the mirror image of the original growth curve is plotted above the new melting curve. The slopes of both lines are in agreement. For comparison, two melting curves starting with ideal crystals at temperatures just below and just above the present temperature are also displayed. Clearly, the old method gives much smaller melting rates. The experiment was repeated for four different temperatures and displayed as squares in Fig. 2. The asymmetry of the interface response has now completely disappeared. This phenomenon has been completely attributed to the subtlety of preparing initial configurations. The much smaller melting rates from the totally ordered crystal might be the reason why Burke et al. [7] failed to produce steady state melting. Instead, their overheating was so large that they reached the mechanical melting point, i.e. the point at which the whole crystal disintegrates at once.

It is important to note that it is not the constant pressure situation (which allows the crystal to relax its volume), but either the presence of an interface or the rapid incorporation of defects during growth which causes the slightly disordered structure. In an earlier paper [8], we showed that the kinetic growth coefficient obtained from nonequilibrium simulations can also be obtained from the fluctuations of the number of crystalline atoms in an equilibrium simulation. In the light of the above, we investigated whether the crystalline phase in such an equilibrium simulation contains an equal number of imperfections as seen in the nonequilibrium simulation. Snapshots of different stages in an extensive equilibrium simulation are shown in Fig. 3. Indeed, the number of imperfections is comparable. Note that the imperfections extend throughout the whole crystal, and not just in the regions where the crystal has melted and regrown during fluctuations. This means that it is the proximity of the liquid phase that causes the slight disorder in the crystal and not just the rapid incorporation of defects.

A more quantitative measure of the disorder is provided in Fig. 5. There we have calculated the BT-profile, as introduced by Jesson and Madden [19], which is the laterally integrated average number density of liquid material. Were the crystal totally ordered, the value would have dropped to zero. For comparison, also the laterally averaged density profile is shown. It can be seen that the density in the liquid and in the solid agree perfectly with the bulk values obtained from the bulk

simulations. This again shows that it is not enough to just look at static bulk properties in order to decide whether equilibrium is reached. We are at present undertaking research to extract the kinetic growth coefficient from the equilibrium simulation in the spirit of Ref. [8].

5. Conclusions

In the present paper, we have investigated the response of the FCC (1 0 0) crystal–liquid interface to small superheatings and undercoolings with respect to the equilibrium melting temperature. This led to an asymmetry of the response, which was explained in terms of lattice imperfections in the crystalline phase. Such imperfections naturally evolved in the growing crystal in contact with a liquid phase, but were absent in the equilibrated bulk crystal and thus also in the melting simulations. When the melting simulations were started from configurations produced during growth of the two-phase systems (thus including imperfections in the crystalline lattice), the asymmetry between growth and melting rates around equilibrium completely disappeared.

Equilibrium simulations of a two-phase system were shown to produce lattice imperfections equivalent to the ones emerging in growth simulations. This implies that equilibrium simulations as advocated in Ref. [8] may provide an alternative for calculating the interface response near equilibrium in a more straightforward manner.

References

[1] K.A. Jackson, J. Crystal Growth 198/199 (1999) 1.
[2] A.C. Levi, M. Korla, J. Phys.: Condens. Mater. 9 (1997) 299.
[3] B.B. Laird, A.D.J. Haymet, Chem. Rev. 92 1992 (1819).
[4] J.Q. Broughton, G.H. Gilmer, K.A. Jackson, Phys. Rev. Lett. 49 (1982) 1496.
[5] J.Q. Broughton, G.H. Gilmer, J. Chem. Phys. 79 (1983) 5095.
[6] J.Q. Broughton, G.H. Gilmer, J. Chem. Phys. 84 (1986) 5749.
[7] E. Burke, J.Q. Broughton, G.H. Gilmer, J. Chem. Phys. 89 (1988) 1030.
[8] W.J. Briels, H.L. Tepper, Phys. Rev. Lett. 79 (1997) 5074.
[9] J.P. Hoogenboom, H.L. Tepper, N.F.A. van der Vegt, W.J. Briels, J. Chem. Phys. 113 (2000) 6875.
[10] D.R. Uhlmann, J.F. Hays, D. Turnbull, Phys. Chem. Glasses 8 (1967) 1.
[11] J.Y. Tsao, M.J. Aziz, M.O. Thompson, P.S. Peercy, Phys. Rev. Lett. 56 (1986) 2712.
[12] M.D. Kluge, J.R. Ray, Phys. Rev. B 39 (1989) 1738.
[13] C.J. Tymczak, J.R. Ray, J. Chem. Phys. 92 (1990) 7520.
[14] R. Moss, P. Harrowell, J. Chem. Phys. 100 (1994) 7630.
[15] J.H.R. Clarke, W. Smith, L.V. Woodcock, J. Chem. Phys. 84 (1986) 2290.
[16] S. Nosé, J. Chem. Phys. 81 (1984) 511.
[17] W.G. Hoover, Phys. Rev. A 31 (1985) 1695.
[18] H.E.A. Huitema, M.J. Vlot, J.P. van der Eerden, J. Chem. Phys. 111 (1999) 4714.
[19] B.J. Jesson, P.A. Madden, J. Chem. Phys. 113 (2000) 5935.